Determination of Aerosol Size Distributions from Lidar Measurements[1]

BENJAMIN M. HERMAN,[2] SAMUEL R. BROWNING[2] AND JOHN A. REAGAN[3]

The University of Arizona, Tucson

(Manuscript received 26 January 1971, in revised form 12 April 1971)

ABSTRACT

It can be shown, theoretically, that the polarization properties of laser light scattered by a volume of air containing aerosols include considerable information as to the size distribution of the aerosols. A theoretical inversion model, utilizing the above information, is developed, which uses the Stokes parameters of the angularly scattered laser light as input data. These input data are generated theoretically from assumed size distribution functions of the aerosols. Both "perfect" measurements and measurements into which random errors are introduced are employed. These data are then used in the inversion model to generate predicted size distribution functions. Numerical experiments are performed with 0, 1 and 2% random error in the observations, in order to determine what accuracy is required in the lidar measurements. Comparisons between the actual and predicted functions are then made in order to assess the accuracy of the model.

1. Introduction

Within recent years, with the development of high-powered, pulsed-laser radar (lidar) systems, considerable effort has been directed toward the problem of utilizing these systems to infer information concerning the vertical structure of the atmosphere (e.g., Fiocco and Smullin, 1963; Collis, 1966; Clemesha *et al.*, 1967). The above studies were based on an analysis of the backscattered signals only, and, as such, were quite limited in information content. Therefore, little progress has been made from such studies toward inferring aerosol size distributions (Barrett and Ben-Dov, 1967). However, as has been pointed out by Reagan *et al.* (1970), considerable additional information can be obtained concerning the angular scattering parameters of the aerosols from the use of bistatic lidar. Accordingly, a bistatic lidar system has been constructed at The University of Arizona for the purpose of studying the size and height distributions of atmospheric aerosols. The essential features of this system have been described elsewhere (Reagan and Herman, 1970; Reagan *et al.*, 1970). This system is unique in that it measures the four Stokes polarization parameters of the angularly scattered light, and the geometry of the system is such that measurements can be obtained from a wide range of scattering angles at a given height.

One of the characteristics of atmospheric aerosols of radius $r>0.1\mu$ which distinguishes them from the molecular, or Rayleigh, component is the fact that, if the incident light is linearly polarized in a direction neither parallel nor perpendicular to the scattering plane, the singly scattered light will exhibit partial elliptical polarization. In addition, the degree of polarization and the plane of polarization of the singly scattered light will also show a marked dependence upon scattering angle and size distribution function which will differ appreciably from that due to the molecular component. It would thus appear that considerable additional information concerning the size distribution function of the aerosols could be obtained through measurements of the polarization parameters of the angularly scattered light, as opposed to measurements of the total intensity only. In the discussion to follow, a theoretical technique is described for inferring the aerosol size distribution function from a given set of simulated measurements of the four Stokes parameters, which can be obtained from such a bistatic lidar system. All calculations assume that the particles are spherical in shape with an index of refraction[4] of 1.54.

[1] The research reported in this article has been supported by the National Aeronautics and Space Administration, under Grant NGR 03-002-155, and the National Science Foundation, under Grant GA 16764.

[2] Institute of Atmospheric Physics.

[3] Department of Electrical Engineering.

[4] It is known that both naturally occurring aerosols and man-made particles are not spherical in shape. Some experimental work on this problem has been carried out by Holland and Draper (1967) and Holland and Gagne (1970) which indicates that there may, in fact, be rather large departures of the scattering parameters from those computed on the basis of spherical particles. On the other hand, Eiden (1966), Bullrich *et al.* (1969), and others have used the spherical assumption and obtained good agreement between theory and observation in studies of the scattering by atmospheric aerosols. Nevertheless, the necessary assumption of spherically shaped particles has been made in the theoretical work to follow, as there are presently no known methods of computing the scattering parameters for randomly oriented arrays of randomly shaped particles. Furthermore, while there is some uncertainty as to the proper value of the index of refraction, a value of about 1.54 appears to be quite typical of a large class of aerosols (Eiden, 1966; Bullrich *et al.*, 1969). Another possible source of error is the possible depolarization of the transmitted pulse by the intervening atmosphere. However, as shown by Höhn (1969), this effect is quite small compared to the effects mentioned above.

2. Theoretical development

Fig. 1 shows a schematic diagram of the bistatic system. In this diagram the transmitter sends out a pulse at an angle γ_1 to the local normal, while the receiver views at an angle γ_2 to the local normal. The darkened area at a height z above the ground represents the instantaneous scattering volume which is that volume from which scattered light, scattered through the angle θ, reaches the receiver at a given instant of time. For the case in which the transmitted pulse is essentially all within the receiver field of view, the lidar equation for the nth Stokes parameter of the singly scattered flux[5] received by the receiver, $F_n^{(s)}(\theta,R_2)$, is

$$F_n^{(s)}(\theta,R_2)=\frac{A_R l}{2R_2^2\sin^2(\theta/2)}\times\exp\left[-\tau(z)\left(\frac{1}{\cos\gamma_1}+\frac{1}{\cos\gamma_2}\right)\right]P_{nm}(\theta)F_m^{(t)};\quad m,n=1,2,3,4, \quad (1)$$

where $\tau(z)$ is the optical depth from the ground to height z, l the pulse length, A_R the effective receiver aperture, and $F_m^{(t)}$ is the mth Stokes parameter of the transmitted flux. The term $P_{nm}(\theta)$ is the nmth element of the scattering matrix for scattering through the angle θ, with dimensions of cross section per unit volume per steradian. For a more complete discussion of the lidar equation, see Reagan and Herman (1970). Since $R_2=z/\cos\gamma_2$, Eq. (1) may be written as

$$F_n^{(s)}(\theta,\gamma_2)=K\frac{\cos^2\gamma_2}{\sin^2(\theta/2)}\times\exp\left[-\tau(z)\left(\frac{1}{\cos\gamma_1}+\frac{1}{\cos\gamma_2}\right)\right]P_{nm}(\theta)F_m^{(t)};\quad m,n=1,2,3,4, \quad (2)$$

where $K=A_R l/(2z^2)$, a constant for observations made at a constant height z.

Let us now consider the scattering matrix element, $P_{nm}(\theta)$. As defined above, this term has the dimensions of scattering cross section per unit volume per steradian and is given by

$$P_{nm}(\theta)=\int_0^\infty P_{nm}(\theta,r)n(r)dr+\frac{\rho(z)}{\rho_0}k_{\lambda 0}P_{nm}(\theta)_{\text{Ray}}, \quad (3)$$

where $P_{nm}(\theta,r)$ is the nmth element of the scattering matrix for a particle of radius r, and $n(r)$ is the particle size distribution function. The term $P_{nm}(\theta)_{\text{Ray}}$ is the nmth element of the normalized scattering matrix for Rayleigh scattering, $k_{\lambda 0}$ the Rayleigh volume attenuation coefficient at some standard level for the wavelength λ, while ρ_0 and $\rho(z)$ are the air densities at the standard level and at the height z, respectively. The integral on the right-hand side can be replaced with a sum, such that Eq. (3) becomes

$$P_{nm}(\theta)\approx P_{nm}(\theta,\bar{r}_1)f(r_1)+P_{nm}(\theta,\bar{r}_2)f(r_2)+\cdots+P_{nm}(\theta,\bar{r}_q)f(r_q)+\frac{\rho(z)}{\rho_0}k_{\lambda 0}P_{nm}(\theta)_{\text{Ray}}, \quad (4)$$

where $P_{nm}(\theta,\bar{r}_j)$ is the nmth element computed at the midpoint radius of the jth interval, and

$$f(r_j)=\int_{r_j}^{r_j+\Delta r_j} n(r)dr;\quad j=1,2,\ldots,q. \quad (5)$$

Substituting (4) into (2), the lidar equation for the nth Stokes parameter at a scattering angle θ_i becomes

$$F_n^{(s)}(\theta_i,\gamma_2)=K\frac{\cos^2\gamma_2}{\sin^2(\theta_i/2)}\times\exp\left[-\tau(z)\left(\frac{1}{\cos\gamma_1}+\frac{1}{\cos\gamma_2}\right)\right]\left[P_{nm}(\theta_i,\bar{r}_1)f(r_1)+P_{nm}(\theta_i,\bar{r}_2)f(r_2)+\cdots+P_{nm}(\theta_i,\bar{r}_q)f(r_q)+\frac{\rho(z)}{\rho_0}k_{\lambda 0}P_{nm}(\theta_i)_{\text{Ray}}\right]F_m^{(t)}. \quad (6)$$

There will thus be four equations of the form of Eq. (6), one for each of the four Stokes parameters (i.e., for each value of $n=1, 2, 3, 4$), for a given angle θ_i. Thus, the total number of such equations will be four times the number of scattering angles at which observations are made. In general, we may write

$$\mathbf{Af}=\mathbf{g}, \quad (7)$$

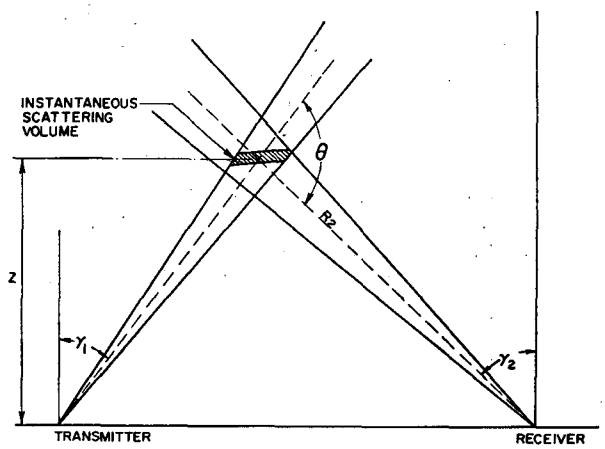

FIG. 1. Schematic diagram of the bistatic lidar system.

[5] It has been shown by Liou and Schotland (1971) that for the bistatic lidar case considered here, when propagating through cloud-free air containing aerosols, the contribution to the scattered flux from secondary and higher order scattering is completely negligible.

where $\mathbf{g}$ is a vector of the observations, with components given by

$$F_n^{(s)}(\theta_i,\gamma_2)-K\frac{\cos^2\gamma_2}{\sin^2(\theta_i/2)}\times\exp\left[-\tau(z)\left(\frac{1}{\cos\gamma_1}+\frac{1}{\cos\gamma_2}\right)\right]\frac{\rho(z)}{\rho_0}k_{\lambda 0}P_{nm}(\theta_i)_{\mathrm{Ray}}F_m^{(t)},$$

and of dimensions $4\times l$, where l is the number of scattering angles θ_i at which observations are made. We have here assumed that the optical depth $\tau(z)$ is known so that the Rayleigh contribution term may be computed and subtracted from the observations. The value of $\tau(z)$ may, in fact, be determined to within $\pm 1\%$ accuracy from other measurements, the technique for which will be described in a later paper. The vector $\mathbf{f}$ is the vector of the unknowns to be solved for, with components $f(r_1)$, $f(r_2)$, ..., $f(r_q)$, where each component gives the number of particles within the particular increment of radius, as given by Eq. (5). The coefficient matrix $\mathbf{A}$ is composed of known quantities, the elements of which are given as

$$\left.\begin{aligned}
A_{11}&=[P_{11}(\theta_1,\bar r_1)F_1^{(t)}+P_{12}(\theta_1,\bar r_1)F_2^{(t)}+P_{13}(\theta_1,\bar r_1)F_3^{(t)}+P_{14}(\theta_1,\bar r_1)F_4^{(t)}]\\
&\qquad\times K\frac{\cos^2\gamma_2}{\sin^2(\theta_1/2)}\exp\left[-\tau(z)\left(\frac{1}{\cos\gamma_1}+\frac{1}{\cos\gamma_2}\right)\right]\\
A_{1q}&=[P_{11}(\theta_1,\bar r_q)F_1^{(t)}+P_{12}(\theta_1,\bar r_q)F_2^{(t)}+P_{13}(\theta_1,\bar r_q)F_3^{(t)}+P_{14}(\theta_1,\bar r_q)F_4^{(t)}]\\
&\qquad\times K\frac{\cos^2\gamma_2}{\sin^2(\theta_1/2)}\exp\left[-\tau(z)\left(\frac{1}{\cos\gamma_1}+\frac{1}{\cos\gamma_2}\right)\right]\\
A_{21}&=[P_{21}(\theta_1,\bar r_1)F_1^{(t)}+P_{22}(\theta_1,\bar r_1)F_2^{(t)}+P_{23}(\theta_1,\bar r_1)F_3^{(t)}+P_{24}(\theta_1,\bar r_1)F_4^{(t)}]\\
&\qquad\times K\frac{\cos^2\gamma_2}{\sin^2(\theta_1/2)}\exp\left[-\tau(z)\left(\frac{1}{\cos\gamma_1}+\frac{1}{\cos\gamma_2}\right)\right]\\
A_{51}&=[P_{11}(\theta_2,\bar r_1)F_1^{(t)}+P_{12}(\theta_2,\bar r_1)F_2^{(t)}+P_{13}(\theta_2,\bar r_1)F_3^{(t)}+P_{14}(\theta_2,\bar r_1)F_4^{(t)}]\\
&\qquad\times K\frac{\cos^2\gamma_2}{\sin^2(\theta_2/2)}\exp\left[-\tau(z)\left(\frac{1}{\cos\gamma_1}+\frac{1}{\cos\gamma_2}\right)\right]\\
A_{4l,q}&=[P_{41}(\theta_l,\bar r_q)F_1^{(t)}+P_{42}(\theta_l,\bar r_q)F_2^{(t)}+P_{43}(\theta_l,\bar r_q)F_3^{(t)}+P_{44}(\theta_l,\bar r_q)F_4^{(t)}]\\
&\qquad\times K\frac{\cos^2\gamma_2}{\sin^2(\theta_l/2)}\exp\left[-\tau(z)\left(\frac{1}{\cos\gamma_1}+\frac{1}{\cos\gamma_2}\right)\right]
\end{aligned}\right\}\quad(8)$$

Thus, the $\mathbf{A}$ matrix will have dimensions $4l\times q$, where $4l$ is the total number of observations, and q the number of unknowns, the $f(r_j)$. The individual elements $P_{nm}(\theta_i,\bar r_j)$ of the $\mathbf{P}$ scattering matrix for a given value of θ and r are determined from Mie theory, while the Stokes parameters of the transmitted light, the $F_n^{(t)}$, are assumed to be $[\frac{1}{2},\frac{1}{2},1,0]$, in order that the transmitted light be linearly polarized at 45° to the scattering plane. This, then, assures that the singly scattered light from aerosols will exhibit elliptical polarization (i.e., $I_4\neq 0$) as described earlier.

In reality, since measurement errors are always present, as are quadrature and roundoff errors in the numerical evaluation of Eq. (3) [e.g., Eq. (4)], Eq. (7) should be written as

$$\mathbf{Af}=\mathbf{g}+\boldsymbol{\varepsilon},\qquad(9)$$

where the components of $\boldsymbol{\varepsilon}$ are the errors in each equation. Because of the presence of errors, Eq. (9) no longer possesses a unique solution, and attempts at a direct solution with $\boldsymbol{\varepsilon}$ set equal to zero almost always result in poor, highly oscillatory solutions, as shown by Phillips (1962). Twomey (1963, 1965) demonstrated possible constraints which are applicable to problems of this sort. One of these constraints is in the form of a smoothing constraint in which the second derivative of the solution points, $\partial^2 f(r_j)/\partial r_j^2$, is minimized. This constraint leads to the solution

$$\mathbf{f}=(\mathbf{A}^T\mathbf{A}+\gamma\mathbf{H})^{-1}\mathbf{A}^T\mathbf{g},\qquad(10)$$

in which $\mathbf{A}^T$ is the transpose of the $\mathbf{A}$ matrix, $\mathbf{H}$ a smoothing matrix, and γ a Lagrangean multiplier. The value of γ determines the amount of smoothing, and is so chosen, by experimentation, to give reasonable solutions. The value of γ is not overly critical, in the sense that varying it from the chosen value over a

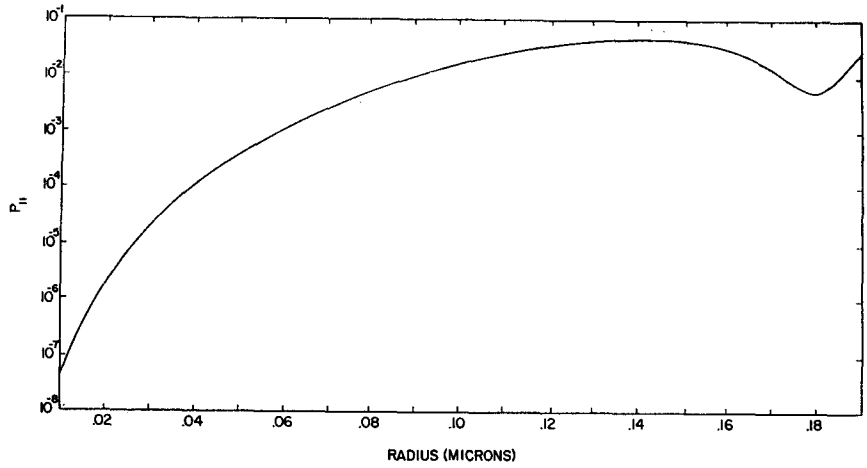

FIG. 2. Scattering matrix element P_{11} for $\theta=130°$, for radii between 0.01 and 0.190 μ.

range of an order of magnitude does not seriously affect the solution.

Another possible constraint proposed by Twomey, for those cases in which a reasonable estimate of the solution is known, consists of minimizing, in a least-squares sense, the differences between the actual solution and the initial estimate, or trial solution. This leads to the solution

$$\mathbf{f}=(\mathbf{A}^T\mathbf{A}+\gamma\mathbf{I})^{-1}(\mathbf{A}^T\mathbf{g}+\gamma\mathbf{P}), \qquad (11)$$

where $\mathbf{I}$ is the identity matrix and $\mathbf{P}$ is the vector of the estimated solution points.

In a later paper, Yamamoto and Tanaka (1969) demonstrated that satisfactory aerosol size distributions from spectral attenuation measurements could be obtained from a combination of the above two methods. Their procedure was to apply the smoothing constraint [Eq. (10)] to get a first solution, and then, using this solution as a trial solution, get a final solution through the use of Eq. (11). A modification of this method was employed in the present work.

In the work of Yamamoto and Tanaka, the elements of the $\mathbf{A}$ matrix were composed of spectral attenuation coefficients which are relatively smooth functions of r. Therefore, in the numerical approximation of their equivalent to (3), relatively large intervals of Δr could be employed. However, in the present study utilizing angular scattering data, the elements of the $\mathbf{A}$ matrix given by Eq. (8) are composed of elements of the scattering matrix, $P_{nm}(\theta,r)$. For values of $r<\lambda$, where λ is the wavelength of the incident light (in this case, 0.6943 μ, representative of a ruby laser), $P_{nm}(\theta,r)$ is indeed a smooth function of r. This is demonstrated in Fig. 2, which shows P_{11} for $\theta=130°$, for radii between 0.01 and 0.190 μ. However, as r increases, the matrix elements become an increasingly erratic function of r, as demonstrated in Fig. 3, which shows the same element for radii between 1.20 and 1.50 μ. Therefore, in order to get an accurate numerical representation of Eq. (3), it is necessary to break the integral up into a large number of very small intervals (Dave, 1969). For the range of sizes considered in this work ($0.025\leqslant r\leqslant 10\,\mu$), approximately 1000 intervals in r were considered necessary, in order to assure a reasonably accurate representation of the integral in (3). This, then, would require 1000 values of the unknown $f(r_j)$, as can be seen from Eqs. (4) and (5), which in turn would require the inverse of a matrix, $\mathbf{A}^T\mathbf{A}$, as in Eqs. (10) and (11), of dimensions 1000×1000. In order to simplify this process, the following technique was employed. Each of the relatively large intervals in Eq. (4) was broken down into a series of smaller sub-intervals, such that Eq. (4) less the Rayleigh term becomes

$$P_{nm}(\theta_i)_{\text{aer}}\approx f(r_1)\sum_{k_1}P_{nm}(\theta_i,\bar{r}_{k1})W_{k1}(r_{k1}) +f(r_2)\sum_{k_2}P_{nm}(\theta_i,\bar{r}_{k2})W_{k2}(r_{k2})+\cdots +f(r_q)\sum_{k_q}P_{nm}(\theta_i,\bar{r}_{kq})W_{kq}(r_{kq}), \qquad (12)$$

where the $W_j(r_j)$ are weighting functions to be described below, and the subscript aer indicates that part of the scattering matrix element due to aerosols only. The coefficients of the unknown $f(\bar{r}_j)$ in Eq. (12) will then appear in the expression for the coefficient matrix, Eq. (8), in place of the $P_{nm}(\theta_i,\bar{r}_j)$. Thus, for example, the expression for A_{11} becomes

$$A_{11}=\Big[\sum_{k_1}P_{11}(\theta_1,\bar{r}_{k1})W_{k1}(r_{k1})F_1^{(l)} +\sum_{k_1}P_{12}(\theta_1,\bar{r}_{k1})W_{k1}(r_{k1})F_2^{(l)} +\sum_{k_1}P_{13}(\theta_1,\bar{r}_{k1})W_{k1}(r_{k1})F_3^{(l)} +\sum_{k_1}P_{14}(\theta_1,\bar{r}_{k1})W_{k1}(r_{k1})F_4^{(l)}\Big] \times K\frac{\cos^2\gamma_2}{\sin^2(\theta_1/2)}\exp\left[-\tau(z)\left(\frac{1}{\cos\gamma_1}+\frac{1}{\cos\gamma_2}\right)\right]. \qquad (13)$$

Initially, the weighting functions are unknown, as knowing them would be equivalent to knowing the sought-after size distribution function. Thus, an "intelligent" first guess is made, and the problem reduces to one of finding the unknown $f(r_j)$ which, when multiplied by the assumed weighting functions, gives the desired size distribution function. If the initially assumed weighting functions are exact, the solution vector **f** will be a unit vector [i.e., $f(r_j)=1$, $j=1, 2,\ldots q$]. Any errors in the initial guess of the weighting function will be mathematically indistinguishable from measurement errors, and, therefore, the worse the initial estimate, the worse will be the resulting solution. However, since this first solution will still be a better approximation than the first guess, the process is repeated. For the second iteration, however, the first solution is used as the weighting function, and a new $f'(r_j)$ is solved for. For the second iteration, the first solution vector components are assumed to be valid at the mid-point of each of the large intervals in r, and are connected by straight lines. Thus, for the second iteration, Eq. (12) becomes

$$P_{nm}(\theta_i)_{\text{aer}}=f'(r_1)\sum_{k_1}P_{nm}(\theta_i,\bar{r}_{k1})\times\left\{f(r_1)+\left[\frac{f(r_2)-f(r_1)}{\Delta r_1}\right]\Delta r_{k1}\right\}W_{k1}(r_{k1})+\cdots+f'(r_{q-1})\sum_{k_{q-1}}P_{nm}(\theta_i,\bar{r}_{kq-1})\times\left\{f(r_{q-1})+\left[\frac{f(r_q)-f(r_{q-1})}{\Delta r_{q-1}}\right]\Delta r_{kq-1}\right\}\times W_{kq-1}(r_{kq-1}), \quad (14)$$

where $\Delta r_1\cdots\Delta r_{q-1}$ are the increments of Δr for the large intervals, the Δr_{kj} are the intervals of Δr in the sub-intervals, and the $f'(r_j)$ are the components of the new solution vector. In principle, one could continue the iterative process until two successive solution vectors agreed to within any prespecified amount. In practice, it was found that two such iterations were adequate, the second such solution then being used as a trial solution, as previously described.

Since most measurements of the size distribution of continental aerosols seem to indicate that these functions follow typically what is known as a Junge distribution (Junge, 1955; Clark and Whitby, 1967), given by

$$\frac{dn}{dr}=cr^{-(\nu^*+1)}, \quad (15)$$

a reasonable first guess for the weighting functions would be to assume that the distribution function is of the form given by Eq. (15). Thus, W_{kj} is given by

$$W_{kj}=\Delta n_{kj}=\int_{r_{kj}}^{r_{kj}+\Delta r_{kj}}cr^{-(\nu^*+1)}dr=\frac{c}{\nu^*}\left[\frac{1}{r_{kj}{}^{\nu^*}}-\frac{1}{(r_{kj}+\Delta r_{kj})^{\nu^*}}\right], \quad (16)$$

where c is a normalizing constant determined such that the total integral of (15) over all sizes yields the proper number density per unit volume, while ν^* is a shaping constant. Typical values of ν^* lie in the range 2.0–4.0.

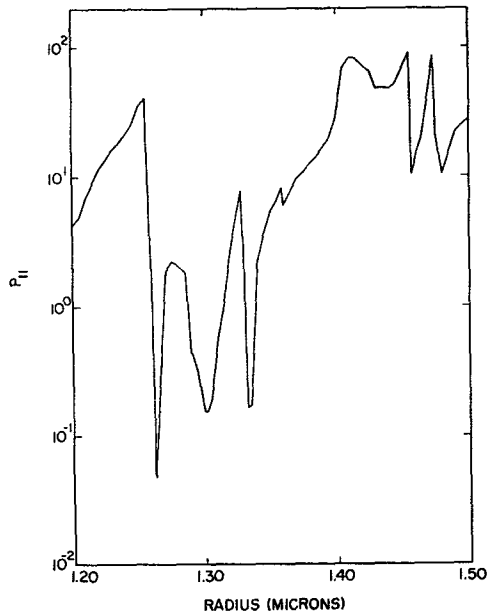

FIG. 3. Scattering matrix element P_{11} for $\theta=130°$, for radii between 1.20 and 1.50 μ.

In the work to follow, "measurements" of the four Stokes parameters at five scattering angles θ, at a fixed height z, and for various assumed size distributions, were computed from Eq. (2.) These 20 "observations" were then used *per se*, and with introduced random errors of 1 and 2%, in order to compute 20 inversion solution points, the $f(r_j)$, by the technique described above. These solution points were taken to apply over each of 20 large intervals in Δr, taken such that log Δr = constant for all intervals. The volume scattering matrix elements due to aerosols, $P_{nm}(\theta)_{\text{aer}}$, were computed from Mie theory with a numerical approximation to Eq. (3), while the Rayleigh component was computed assuming a standard atmospheric density distribution.

3. Discussion of results

Fig. 4 shows an inversion solution for a true distribution which is a straight Junge type with $\nu^*=2.5$. The initial weighting functions were computed from

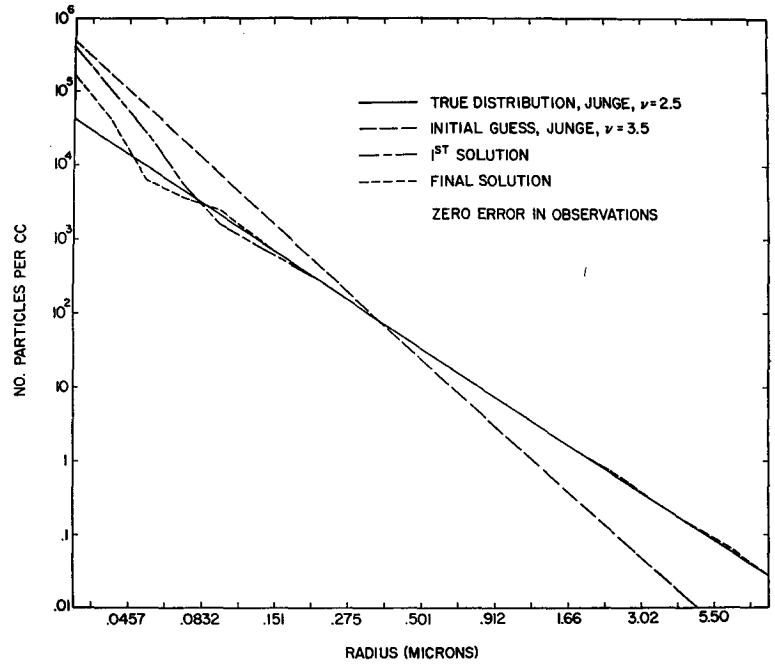

FIG. 4. Inversion solution for a Junge distribution with $\nu^*=2.5$, with an initial guess of $\nu^*=3.5$ and zero error in the observations.

Eq. (16) assuming $\nu^*=3.5$ (long dashes). The initial smoothing solution, Eq. (10), is shown as short and long dashes, while the final solution, Eq. (11) is shown as short dashes. For the sake of clarity, the second iteration using the smoothing constraint has been omitted from this figure and from Fig. 5, but in both cases it lies roughly intermediate between the first and final solutions. In this case, a nearly perfect inversion is obtained for radii $\gtrsim 0.2\ \mu$. It is important to note here that "exact observations" were used in this case; that is, observations precisely as computed were used. In the smaller range of sizes, results, while satisfactory, are not quite as good. This is undoubtedly due to the fact that the smaller sizes are in the Rayleigh region for the ruby wavelength, which results in all such particles having the same variation of the scattering matrix elements with scattering angle θ. Thus, the only information content in the measurements for these small particles, if they were precisely Rayleigh scatterers, is the total scattering cross section, and this can be made

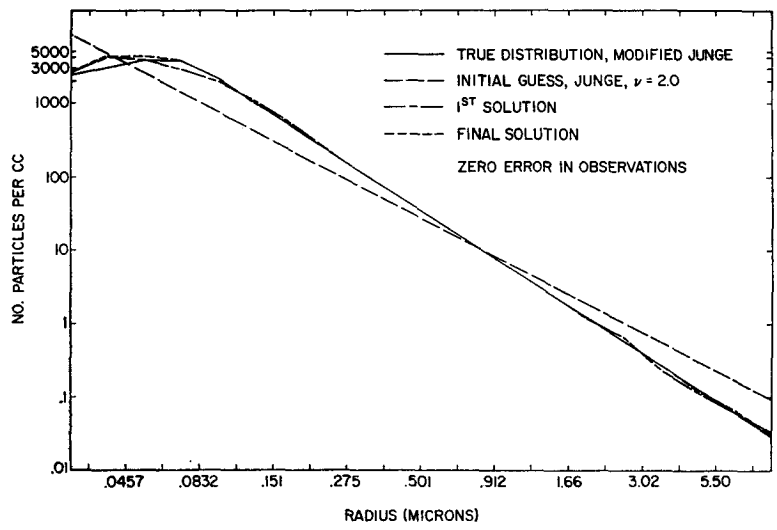

FIG. 5. Inversion solution for a modified Junge or X distribution (see text), with an initial guess of $\nu^*=2.0$ and zero error in the observations.

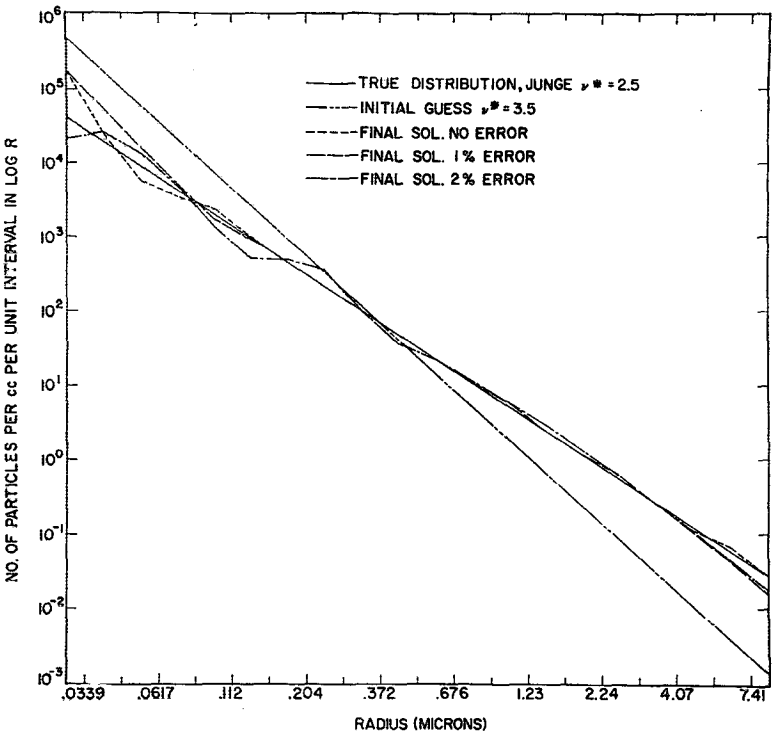

FIG. 6. Inversion solutions for a Junge distribution with $\nu^*=2.5$, with zero, 1% and 2% errors in the observations.

up of large numbers of the smallest particles, or fewer numbers of the larger particles of the Rayleigh region, or any intermediate distribution. Since the scattering differs slightly from pure Rayleigh, there is, in fact, a slight amount of information content in the measurements, as can be seen from Fig. 5. In this figure, the true distribution of particles is a modified Junge distribution (called distribution X), in which a parabola, given by $dn/dr=a(r_1-r)^2+b$, was assumed for $r\leqslant 0.103$ μ and a Junge distribution with $\nu^*=2.5$ was assumed for $r\geqslant 0.103\,\mu$. The constants a and b were determined by setting dn/dr and $d/dr(dn/dr)$ equal for both distributions at $r=0.103\,\mu$. As an initial guess for the weighting functions, a straight Junge distribution with $\nu^*=2.0$ was employed. Again, zero error was placed in the observations. As can be seen from the figure, an excellent solution resulted, even at the smaller sizes where the distribution departed markedly from a Junge type.

Figs. 6-8 present results in which random errors of 1 and 2% were put into the observations, in addition to the "zero error" results. For the sake of clarity, only the final solutions are shown. Fig. 6 is for a straight Junge distribution with $\nu^*=2.5$. As can be seen, the presence of errors up to 2% degrades the solution only slightly, and, in general, the results show excellent agreement between the true and computed distributions. Fig. 7 shows the results for distribution X, except that a much worse initial guess of $\nu^*=4.5$ was used as compared with the results shown in Fig. 5. By comparison of the final solution with no error in Fig. 7 to the final solution of Fig. 5, it can be seen that this worse initial guess definitely leads to a poorer final solution, particularly at the smallest sizes. Even so, the final solutions

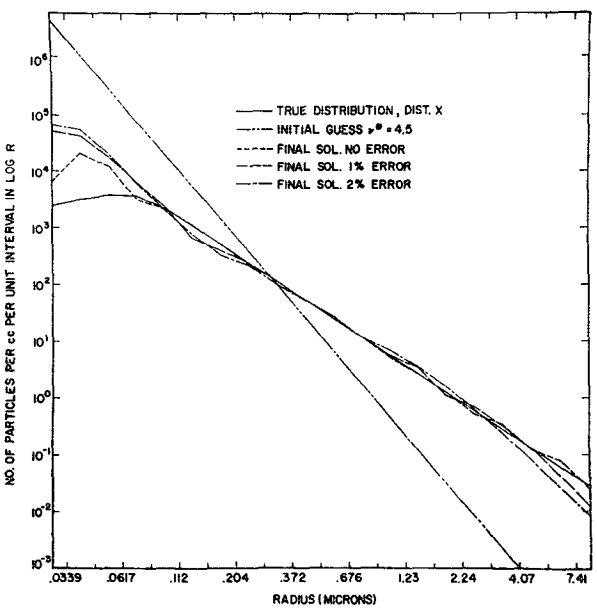

FIG. 7. Same as Fig. 6 except for distribution X.

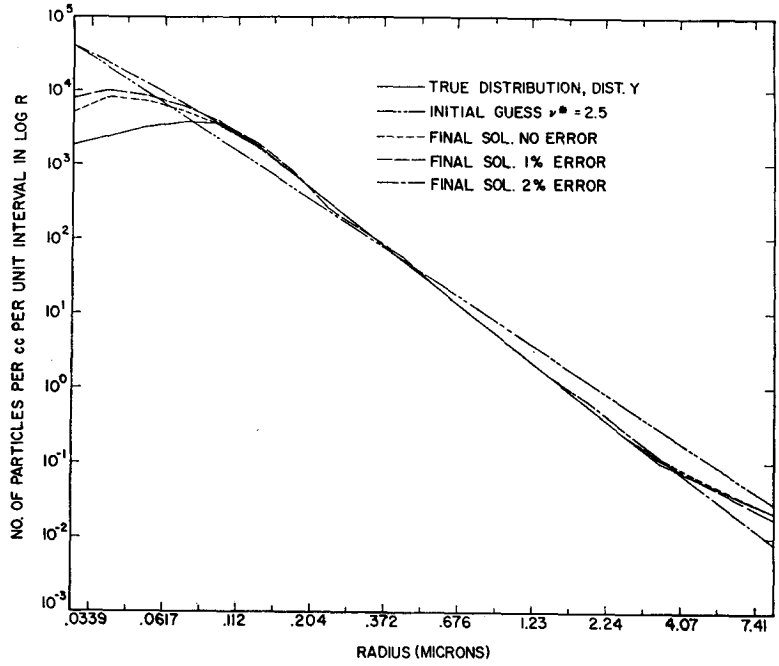

FIG. 8. Same as Fig. 6 except for distribution Y.

must be considered as quite satisfactory, with no appreciable degradation with the introduction of measurement errors, except again at the smaller sizes. Apparently the introduction of even small errors into the observations is enough to essentially eliminate all information content about the smallest sizes, due to the initially low content inherent in these sizes as previously discussed.

Finally, in Fig. 8, results are presented for another distribution, distribution Y. For this distribution, a parabola of the same form as that used in distribution X was used for $r \leqslant 1.3\,\mu$. This was fitted to a Junge distribution with $\nu^* = 3.0$ for $1.3\,\mu \leqslant r \leqslant 3.4\,\mu$, while for $r \geqslant 3.4\,\mu$ a Junge distribution with $\nu^* = 1.1$ was assumed. The results again are considered quite satisfactory. For zero error and 1% error, it is noted that the solution is able to follow the abrupt change in slope at $3.4\,\mu$, while with 2% error, the constraint required [i.e., the value of γ in Eqs. (10) and (11)] is large enough so as to force the solution into a nearly straight line on the log-log plot of the figure. This is true at the small-size end of the distribution also. Here, the zero and 1% error solutions are able to somewhat follow the curvature of the true solution, but with 2% error this feature is completely lost.

Considerable experimentation yet remains to be done. The effect of variations in the index of refraction requires further study. Also, the ability of the method to reproduce size distributions which deviate greatly from the Junge types employed here has not been investigated nor has the effect of changing the upper and lower limits of particle radius solved for in the inversion. Finally and perhaps most serious are the effects of the non-spherical shapes of real aerosols. Some of this work is currently under investigation and will be reported upon at a later date.

REFERENCES

Barrett, E. W., and O. Ben-Dov, 1967: Application of lidar to air pollution measurements. *J. Appl. Meteor.*, **6**, 500–515.

Bullrich, K., R. Eiden, G. Eschelbach, K. Fischer, G. Hänel, K. Heger, H. Schollmayer and G. Steinhorst, 1969: Research on atmospheric optical radiation transmission. Institut für Meteorologie der Johannes Gutenberg-Universität, Mainz, Germany, Sci. Rept. No. 7, AFCRL Contract F61052 67C 0046, 111 pp.

Clark, W., and K. Whitby, 1967: Concentration and size distribution measurements of atmospheric aerosols and a test of the theory of self-preserving size distributions. *J. Atmos. Sci.*, **24**, 677–687.

Clemesha, B. R., G. S. Kent and R. W. H. Wright, 1967: A laser radar for atmospheric studies. *J. Appl. Meteor.*, **6**, 386–395.

Collis, R. T. H., 1966: Lidar: A new atmospheric probe. *Quart. J. Roy. Meteor. Soc.*, **92**, 220–230.

Dave, J. V., 1969: Effect of coarseness of the integration increment on the calculation of the radiation scattered by polydispersed aerosols. *Appl. Opt.*, **8**, 1161–1167.

Eiden, R., 1966: The elliptical polarization of light scattered by a unit volume of atmospheric air. *Appl. Opt.*, **5**, 569–575.

Fiocco, G., and L. Smullin, 1963: Detection of scattering layers in the upper atmosphere (60–140 km) by optical radar. *Nature*, **199**, 1275–1276.

Höhn, D. H., 1969: Depolarization of a laser beam at 6328 Å due to atmospheric transmission. *Appl. Opt.*, **8**, 367–369.

Holland, A. C., and J. S. Draper, 1967: Analytical and experimental investigation of light scattering from polydispersions of Mie particles. *Appl. Opt.*, **6**, 511–518.

——, and G. Gagne, 1970: The scattering of polarized light by polydisperse systems of irregular particles. *Appl. Opt.*, **9**, 1113–1121.

Junge, C., 1955: The size distribution and ageing of natural aerosols as determined from electrical and optical data on the atmosphere. *J. Meteor.*, **12**, 13–25.

Liou, K. N., and R. A. Schotland, 1971: Multiple backscattering and depolarization from water clouds for a pulsed lidar system. *J. Atmos. Sci.*, **28**, 772–784.

Phillips, B. L., 1962: A technique for the numerical solution of certain integral equations of the first kind. *J. Assoc. Comp. Mach.*, **9**, 84–97.

Reagan, J. A., and B. M. Herman, 1970: Bistatic lidar investigations of atmospheric aerosols. *Preprints of Papers, Proc. 14th Conf. Radar Meteor.*, Tucson, Ariz., Amer. Meteor. Soc., 275–280.

- · —, —— and R. J. Spiegel, 1970: On the use of bistatic lidar in the study of atmospheric aerosols. *Proc. 1970 Southwest IEEE Conf.*, Dallas, Tex., 526–530.

Twomey, S., 1963: On the numerical solution of Fredholm integral equations of the first kind by the inversion of the linear system produced by quadrature. *J. Assoc. Comp. Mach.*, **10**, 97–101.

——, 1965: The application of numerical filtering to the solution of integral equations encountered in indirect sensing measurements. *J. Franklin Inst.*, **279**, 95–109.

Yamamoto, G., and M. Tanaka, 1969: Determination of aerosol size distribution from spectral attenuation measurements. *Appl. Opt.*, **8**, 447–453.